Bistatic measurement of atmospheric aerosol distributions by using an imaging lidar

Ikue Kouga[1], Yohei Yamaguchi[1], Shunsuke Fukagawa[1], Nobuo Takeuchi[1], Hiroaki Kuze [1], Makoto Sasaki [2], Yoichi Asaoka [2], Satoru Ogawa [3]

[1] Center for Environmental Remote Sensing (CEReS), Chiba University; [2] Institute for Cosmic Ray Research, University of Tokyo; [3] Faculty of Science, Toho University

kouga@graduate.chiba-u.jp

Abstract

Bistatic imaging lidars have unique features, compared with monostatic lidars for detecting backscattering photons. In this study, we describe the measurement of atmospheric aerosol distributions by using two types of bistatic configurations. A new gate scheme based on the GPS signal is proposed and demonstrated. All-sky Survey High Resolution Air-shower (Ashra) telescope has been developed to detect UV emissions in the atmosphere produced by ultra-high energy cosmic-ray particles. The application of this Ashra telescope technique to atmospheric monitoring enables us to carry out nearly real-time monitoring of the two-dimensional distributions of aerosols and clouds.

1. Introduction

The All-sky Survey High Resolution Air-shower (Ashra) telescope project has been developed by University of Tokyo for the purpose of detecting high-energy cosmic rays (http://www.icrr.u-tokyo.ac.jp/~ashra/index-e.html). In this project, the Chiba University group is in charge of application of the Ashra telescope to the monitoring of the atmosphere. This telescope accomplishes a wide field-of-view (FOV) (50×50 deg) with no need for scanning its optics. Also, the system realizes a high angular resolution (1 arcmin = 0.29 mrad) and a high-speed, highly sensitive imaging with an intelligent triggering capability [1,2]. In the present paper, the imaging lidar is operated in the bistatic mode, in which the telescope is placed at a certain distance from the laser location.[3] The light scattered in the atmosphere is detected in the scattering-angle range of $0<\theta<180$ deg. Although bistatic measurements of aerosols and clouds have so far been reported[5-9], the detection schemes were mainly for the detection of backscattering photons, with little attempt of scanning the laser beam in the detector FOV. Compared with the backscatter signal, forward scattering yields high signal-to-noise ratio (SNR) owing to the general property of the Mie scattering from aerosols. In the present measurement, another advantage is the use of the precise gate system that is based on the 1 pulse-per-second (PPS) signal of the GPS system. This greatly contributes to reduce the background light and thereby increases the SNR.

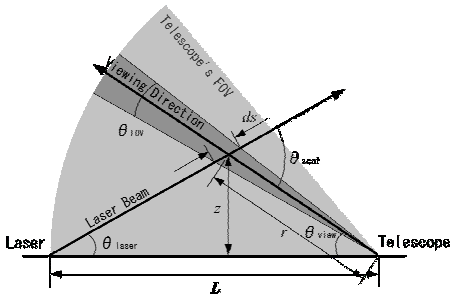

Fig.1 Schematic diagram of the bistatic measurement.

2. Bistatic measurement of aerosol

The basic configuration of the bistatic measurement is shown in Fig. 1. A laser and a telescope are located separately, with a baseline distance of L. The laser is illuminating a direction θ_{laser} in elevation, while the telescope is observing the beam path toward a direction θ_{view}. In this bistatic measurement, the lidar equation is written as

$$P = P_0 \; K \; \frac{A}{r^2} \; ds \; \beta\left(\theta_{\mathrm{scat}}\right) T \; , \qquad (1)$$

where P is the received signal intensity, P_0 the emitted laser intensity, K the efficiency of the receiving optics, A the area of the telescope mirror, r the distance between the target (aerosol particle) and the telescope, θ_{scat} the

scattering angle, and T the transmittance along the combined laser path and viewing path. The portion of the laser beam path subtended by the FOV of a single pixel of the imaging detector (θ_{FOV}) is denoted as ds, which is given as

$$ds = \frac{r\ \theta_{FOV}}{\sin(\theta_{scat})}. \qquad (2)$$

The generalized scattering coefficient, $\beta(\theta_{scat})$, is defined as

$$\beta(\theta_{scat}) = \alpha_1\ f_1(\theta_{scat}) + \alpha_2\ f_2(\theta_{scat}). \quad (3)$$

Here, α_i is the extinction coefficient, and f the phase function. Subscript 1 stands for aerosol and 2 for air molecule.

3. Bistatic lidar measurement

The Ashra telescope is designed for the operation in the UV region, in order to measure the atmospheric emission of air showers. This choice of the wavelength also has the advantage of the eye-safe operation for the imaging lidar system. Since the 1/3-scale model (with a diameter 60 cm for the main mirror) is preparatory for the eventual use of the Ashra telescope, here we report on our recent experiments of the bistatic lidar measurement conducted using cooled CCD cameras (SBIG ST7X and Bitran, BN-51LN) and a pulsed Nd:YAG laser (532 nm).

Two configurations of the bistatic measurements have been tested (Fig. 2). The first case (Fig. 2(a)) is the "in-plane" measurement, in which the laser beam is scanned in a vertical plane that includes both the transmitter and receiver setups. The second case (Fig. 2(b)) is the "cross-plane" measurement, in which the laser beam is scanned in a vertical plane that is almost perpendicular to the viewing direction. In both configurations, it is possible to obtain the monostatic lidar data simultaneously by employing another receiver telescope at the laser site. Parameters of the experiments are summarized in Table 1.

3.1 In-plane observation

The experiment was conducted on the rooftop of a 9-story building on the campus of Chiba University. The

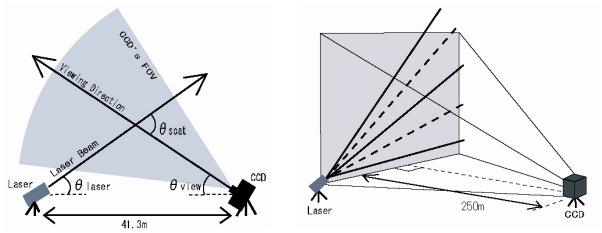

(a) (b)

Fig.2 Schematic diagram of a bistatic imaging lidar measurement (a) In-plane observation, and (b) Cross-plane observation

Table.1 System parameters

Bistatic configuration	In-plane observation	Cross-plane observation
Date	Nov. 25, 2004	Sep.3,2005
Laser	Nd:YAG 532nm	Nd:YAG 532nm
Repetition rate [Hz]	10	10
Power [mJ]	30	100
Cooled CCD	SBIG ST7X	Bitran-BN51LN
Number of pixels	765×510	400×2672
FOV [deg]	46 (for 765 pixels)	39 (for 4008 pixels)
Q.E.(@ 532 nm)	0.65	0.47
A/D converter[bit]	16	16

baseline distance was 41 m. While fixing the viewing direction of the CCD camera, the elevation angle of the laser emission was changed in an angular range of 1-90 deg. The *s*-polarization direction of the laser beam was chosen so that the angular dependence of the Rayleigh scattering component was minimized.

Figure 3 shows the result of this in-plane measurement. In Fig. 3(a), the received signal intensity (as received and not range-corrected) is plotted in a two-dimensional diagram. As seen from this figure, the received intensity is larger for the forward scattering at smaller scattering angles. We apply an algorithm to derive the two-dimensional distribution of the aerosol extinction coefficient.[3] Starting from a certain distribution of the aerosol profile near the ground level, we derive the extinction profile point by point toward higher altitudes on the basis of the intensity of lidar return signal. Then, the improved transmission is determined from this tentative extinction profile, and the algorithm is operated

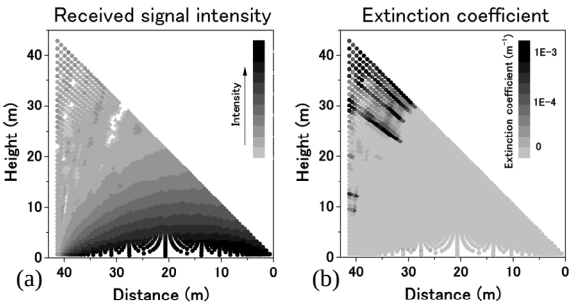

Fig.3 Two-dimensional distribution of
(a)the received signal intensity,
and (b) the extinction coefficient

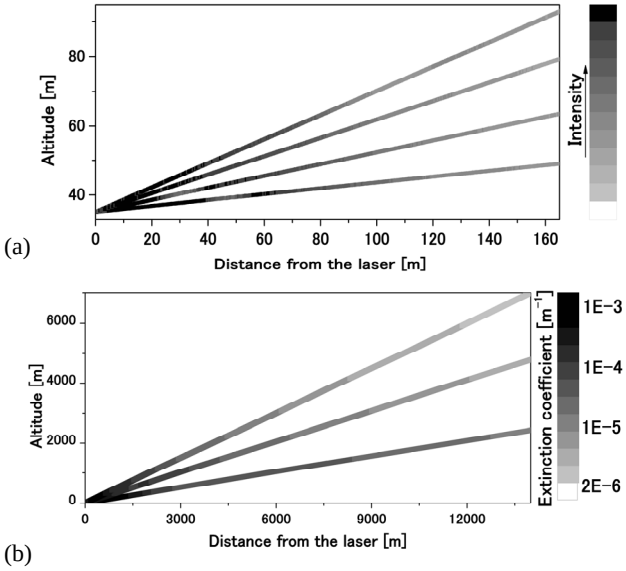

Fig.4 Two-dimensional distribution of
(a) the cross-plane, bistatic measurement,
and (b) monostatic measurement

in an iterative way. We make use of the additional information on aerosol properties measured using ground sampling instruments, including an integrated nephelometer, an optical particle counter, and a homemade scatterometer based on an integrating sphere with two laser beams.[10] The result of this analysis is depicted in Fig. 3(b), which indicates the presence of an aerosol-rich region presumably ascribable to the exhaust plume from the stack on the rooftop.

3.2 Cross-plane observation

In the cross-plane measurement, the laser apparatus is placed on the rooftop of the same building as the in-plane measurement, whereas the CCD camera was placed on the rooftop of another 8-story building, about 300 m away from the laser site. The elevation angle of the laser beam was changed between 5-20 deg, with steps of 5 deg. Figure 4(a) shows the distribution of the scattered light intensity, and Fig. 4(b) shows the distribution of the aerosol extinction coefficient derived from the monostatic measurement simultaneously undertaken. The signal of the monostatic measurement has been analyzed with the standard two-component (aerosols and air molecules) algorithm. By comparing the distributions in Fig. 4(a) and (b), the obvious advantage of the cross-plane, bistatic measurement is its capability of obtaining the aerosol distribution near the ground level, which is usually hindered in the traditional, monostatic measurement due to the overlapping between the laser beam and the telescope FOV. Because of the limited sensitivity of the present detection system using a CCD camera, the profile in Fig. 4(a) was taken in a time period of about 1 h. The use of Ashra telescope would contribute to shorten the measurement duration, since it enables more sensitive detection of the laser beam traces. Another important technique for the improvement of SNR is provided by means of an appropriate gate system, as explained in the next subsection.

4. Trigger synchronization system

An effective method to improve the SNR in the bistatic lidar measurement is the application of the gated detection. By limiting the exposure time of the detector to the precise moment of the passage of the laser beam in the viewing field, it is possible to extract the laser beam image having a high contrast against the background. In the present measurement, we have developed a trigger synchronization system (TSS) that exploits the 1 PPS signal from the GPS system. A schematic diagram of the TSS operation is illustrated in Fig. 5. By comparing the operation of two GPS systems separated by about 10 m, we have ensured that the gate timing can be synchronized with an accuracy of ± 1 μs. Additionally, a peripheral interface controller (PIC) is employed to generate a 3 kHz pulse train for controlling the laser emission.

In the cross-plane measurement mentioned above, a gated image intensifier (Hamamatsu, C9547-03) was installed in front of the cooled CCD camera. Figure 6

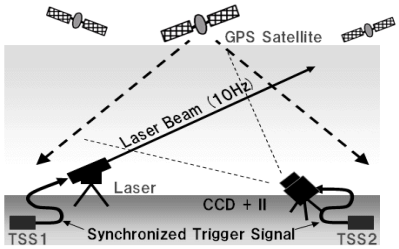

Fig.5 A schematic diagram of the TSS operation

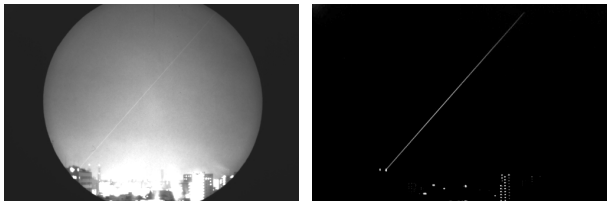

(a) (b)

Fig.6 Images obtained from the cross-plane observation: (a) continuous mode, and (b) gated mode with a gate width of 250 μs, exposure time 2s, repetition rate 10Hz, binning of CCD 4×4

compares the images without (Fig. 6(a)) and with (Fig,6(b)) the gating, with an opening duration of 250 μs. As compared with the background light intensity in the city area, the improvement of SNR is from about 2 to 20.

5. Conclusion

In this paper, we have described the bistatic lidar measurements using two types of configurations. As compared with the traditional approach of the monostatic measurement, the in-plane type of the bistatic measurement has the advantage of enabling the measurement near the forward scattering scheme, which gives much stronger signal than the backscattering measurement. In the case of cross-plane configuration, it is feasible to measure the aerosol distribution from the vicinity of the ground level to upper levels. We are going to investigate the capabilities of the Ashra imaging telescope in the environmental application of real-time, two-dimensional measurement of aerosol and cloud profiles.

Acknowledgment

The financial supports from the Frontier Program of the Japan Promotion of Science and Technology Fund and the grant from the Ministry of Education, Culture, Sports, Science and Technology are gratefully acknowledged.

References

1 M. Sasaki, A. Kusaka, Y. Asaoka, Design of UHECR telescope with 1 arcmin resolution and 50° field of view, Nucl. Instr. Meth. Phys. Res. A492, 49-56 (2002).

2 M. Sasaki, Y. Asaoka, M. Jobashi. Self-triggered image intensifier tube for high-resolution UHECR imaging detector, Nucl. Instr. Meth. Phys. Res.A 501. 359-366 (2003).

3 H. Kuze, S. Fukagawa, N. Takeuchi, Y. Asaoka, and M. Sasaki, “Development of a wide-area imaging lidar for atmospheric monitoring,” 29th SICE Remote Sensing Symposium, 61-64 (2003). (in Japanese)

4 S. Fukagawa, I. Kouga, H. Kuze, N. Takeuchi, M. Sasaki, Y. Asaoka, S. Ogawa, Simulation study for aerosol distribution retrieval from bistatic, imaging lidar data. CLEO/PR2005(Tokyo), C15, (2005).

5 J.A. Reagan, D.M. Byrne, B. Herman, Bistatic LIDAR: a tool for characterizing atmospheric particles:part II- the inverse problem, IEEE Transactions on Geoscience and Remote Sensing, 20, 236-243 (1982).

6 K. Meki, K. Yamaguchi, X. Li, Y. Saito, T.D. Kawahara, and A. Nomura. Range-resolved bistatic imaging lidar for the measurement of the lower atmosphere. Opt. Lett., 21. 1318-1320 (1996).

7 S.P. Love, A.B. Davis, C. Ho, C.A. Rohde, Remote sensing of cloud thickness and liquid water content with wide-angle imaging lidar, Atmos. Res. 59-60. 295-312 (2001).

8 A. Ohzu, K. Akaoka, Y. Maruyama, Performance of a remote particle counter using an imaging lidar system, Extended Abstracts of the 64th meeting of the Jpn. Soc. Appl. Phys. and Related Soc., 2a-ZC-11 (2003) (in Japanese).

9 J.E. Barnes, S. Bronner, R. Beck, N.C. Parikh, Boundary layer scattering measurements with a charge-coupled-device camera lidar, Appl. Opt. 42, 2647-2652 (2003).

10 S. Fukagawa, H. Kuze, N. Lagrosas, N. Takeuchi, High-efficiency aerosol scatterometer that uses an integrating sphere fro the calibration of multiwavelength lidar data, Applied Optics, 44(17), 3520-3526 (2005)